Cell Reports, Volume *24*

Supplemental Information

Von Hippel-Lindau Protein Is Required for Optimal Alveolar Macrophage Terminal Differentiation, Self-Renewal, and Function

Helena M. Izquierdo, Paola Brandi, Manuel-José Gómez, Ruth Conde-Garrosa, Elena Priego, Michel Enamorado, Sarai Martínez-Cano, Iria Sánchez, Laura Conejero, Daniel Jimenez-Carretero, Silvia Martín-Puig, Martin Guilliams, and David Sancho

SUPPLEMENTAL INFORMATION

Figures S1-S3

Supplemental Experimental Procedures

Supplemental References

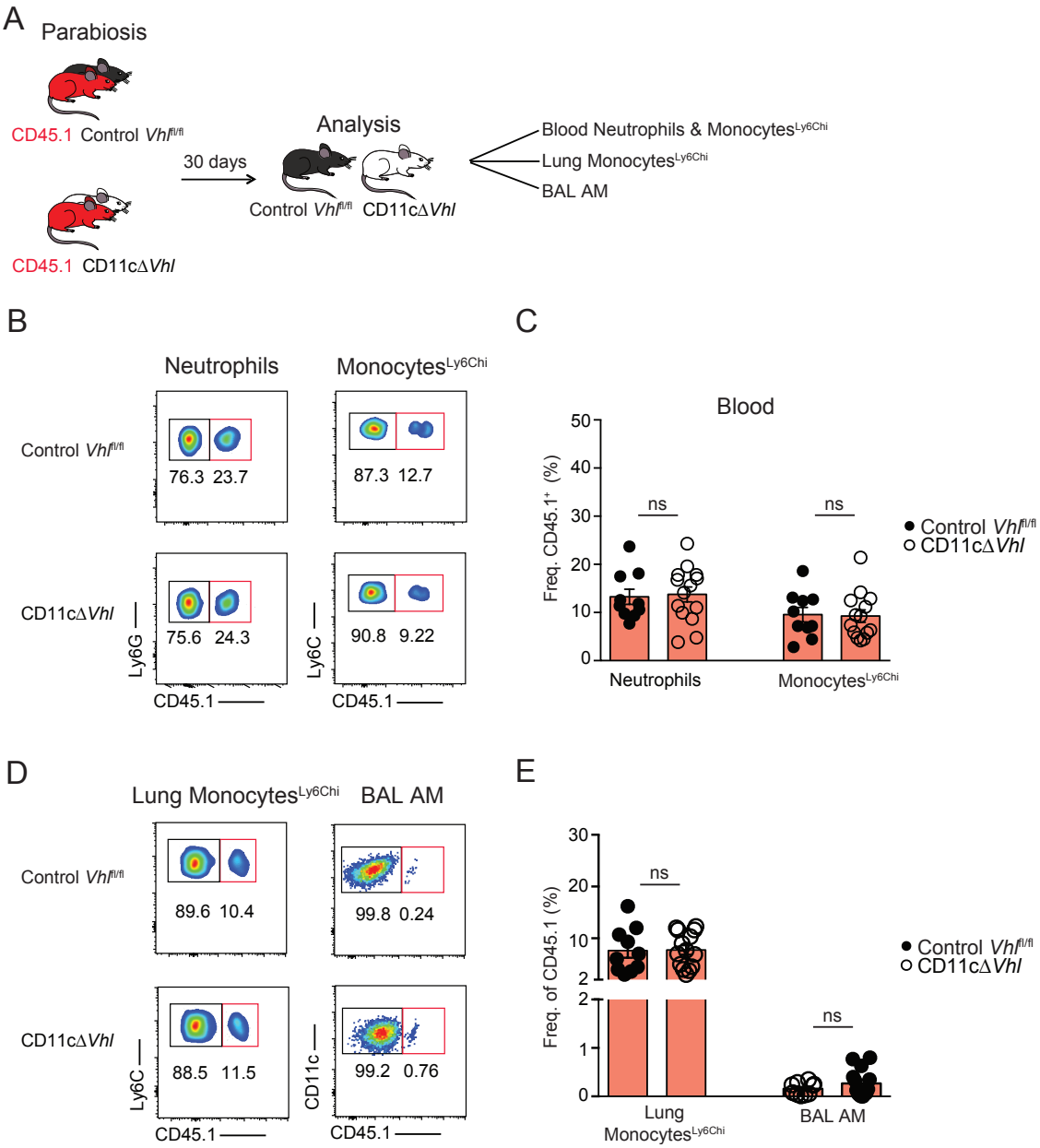

Figure S1. Circulating monocytes do not contribute to Vhl-deficient AM phenotype. Related to Figure 2.
(A) Scheme of parabiosis: CD45.2 control *Vhl*$^{fl/fl}$ and CD11cΔ*Vhl* mice were surgically joined to a CD45.1 mouse in parabiosis. Thirty days after surgery, CD45.2 parabionts were analyzed.
(B, C) Representative flow cytometry plots (B) and frequencies of CD45.1$^+$ cells (C) in neutrophils (gated on CD11b$^+$Ly6G$^+$) and Ly6C^{hi} monocytes (gated on CD11b$^+$Ly6C^{hi}) from peripheral blood.
(D, E) Representative flow cytometry plots (D) and frequencies of CD45.1$^+$ cells (E) in lung Ly6C^{hi} monocytes (gated on CD45$^+$ Siglec-F$^-$ CD11b$^+$ Ly6C^{hi}) and BAL AMs (gated on Siglec-F$^+$ CD11c$^+$).
(C, E) Frequencies shown as mean ± s.e.m. of a pool of three independent experiments performed, where each dot represents an individual mouse (n=10-14 per genotype): ns, not significant (unpaired Student *t*-test).

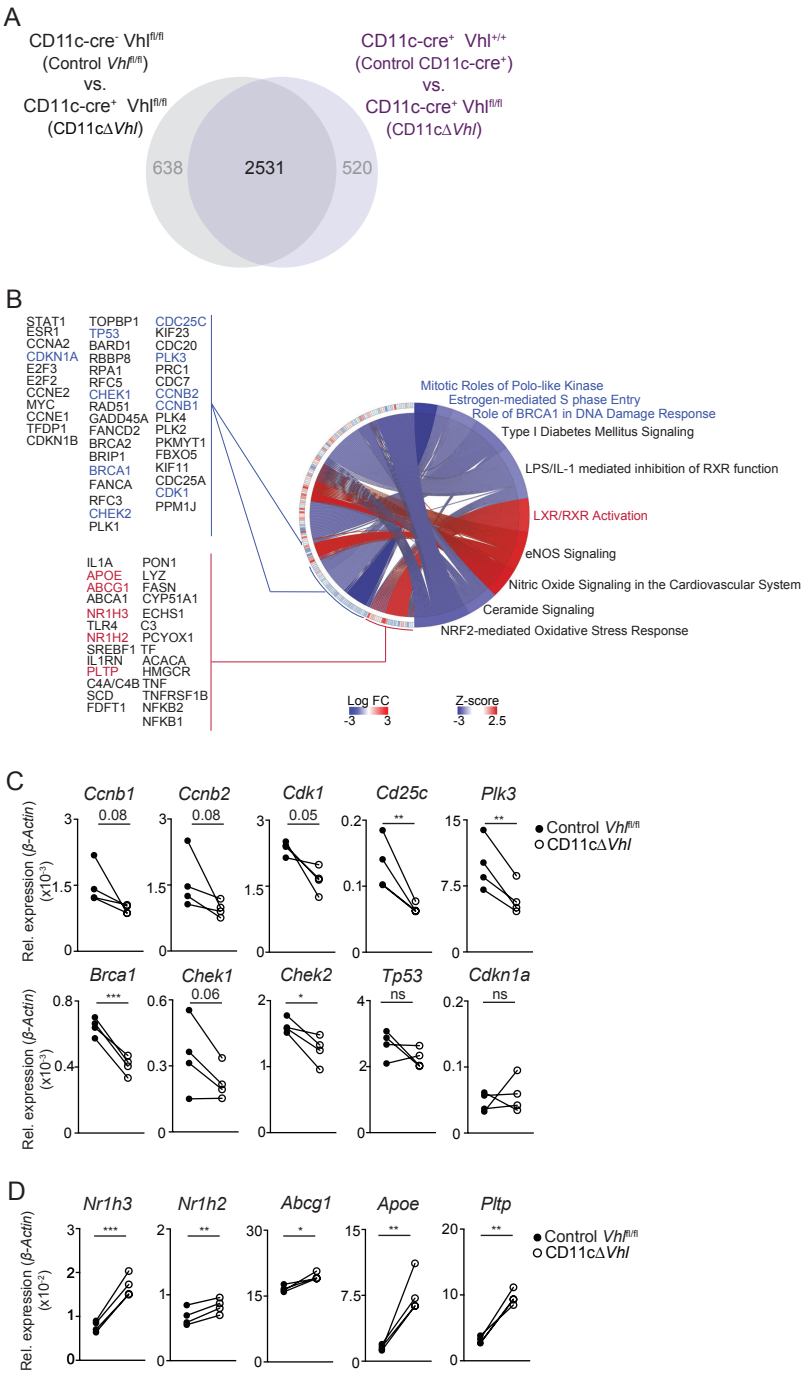

Figure S2. VHL-deficient AMs have an altered gene expression profile. Related to Figures 3 and 4.

(A) Venn diagram showing genes differentially expressed in CD11cΔ*Vhl* AMs versus control *Vhl*$^{fl/fl}$ AMs or control CD11c-cre^{+}.

(B) Circular plot representing Ingenuity Pathway Analysis of differentially expressed genes from pathways with |Z-score| > 2 and -log (B-H p-value) >2.5 in VHL-deficient AMs (CD11cΔ*Vhl*) versus control *Vhl*$^{fl/fl}$ AMs from BAL. Depicted genes correspond to cell-cycle-related (blue) and lipid-handling-related (red) pathways.

(C,D) Quantitative PCR of selected differentially expressed genes related to cell cycle (C) and lipid sensing (D), depicted in blue and red, respectively, in Figure S2B. ns, not significant; *p-value<0.05; **p-value<0.01; ***p-value<0.001 by ratio paired Student *t*-test.

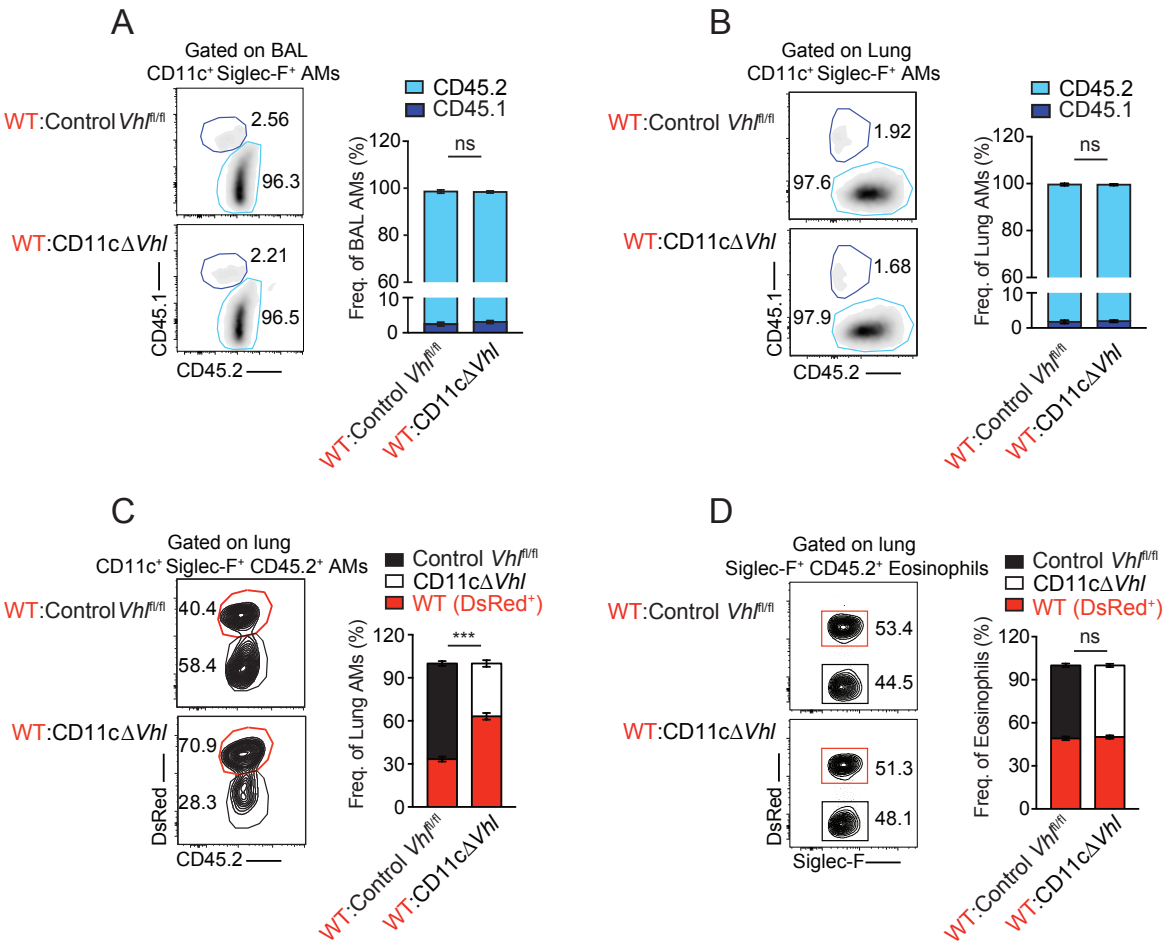

Figure S3. VHL-deficient AMs have a cell autonomous defect in lung reconstitution. Related to Figure 3.
(A-B) Representative flow cytometry plots and frequencies of host CD45.1$^+$ cells and donor CD45.2$^+$ cells in BAL AMs (A) and lung AMs (after BAL) (B) from BM chimeras.
(C-D) Representative flow cytometry plots and frequencies of DsRed$^+$ (WT) and DsRed$^-$ (Control *Vhl*$^{fl/fl}$ or CD11cΔ*Vhl*) cells (normalized to blood Ly6Chi monocyte frequency in each mouse and genotype) in CD45.2$^+$ lung AMs (C) and lung eosinophils (D) from BM chimeras. Frequencies shown as mean ± s.e.m. of one experiment of three independent experiments performed (n=5-10 per genotype): ns, not significant; ***p-value<0.001 by ratio paired Student *t*-test.

SUPPLEMENTAL EXPERIMENTAL PROCEDURES

Quantitative-qPCR

Quantitative PCR was performed in a 7900-FAST-384 instrument (Applied Biosystems) by using the GoTaq qPCR master mix from Promega (Madison, WI)

Primers used in this work (synthetized by Sigma) were as follows: *β-actin* Fw: 5′-GGCTGTATTCCCCTCCATCG-3′, *β-actin* Rv: 5′-CCAGTTGGTAACAATGCCATGT-3′, *Vhl* Fw: 5′-TGTGCCATCCCTCAATGTCG-3′, *Vhl* Rv: 5′-CTTCCGCACACTGGGTAGT-3′, *Slc2a1*Fw: 5′-GGGCATGTGCTTCCAGTATGT-3′, *Slc2a1* Rv: 5′-ACGAGGAGCACCGTGAAGAT-3′, *Ldha* Fw: 5′-TGTCTCCAGCAAAGACTACTGT-3′, *Ldha* Rv: 5′-GACTGTACTTGACAATGTTGGGA-3′, *Arg1* Fw: 5′-CTCCAAGCCAAAGTCCTTAGAG-3′ , *Arg1* Rv: 5′-AGGAGCTGTCATTAGGGACATC-3′, *Itgax* Fw: 5′-AGTGCTAGGGGACGTGAATG-3′, *Itgax* Rv: 5′-TCTGGGATGCTGAAATCCTC-3′ , *Siglec5* Fw: 5′-TTACCTGGCACTGGTGTTACTG-3′, *Siglec5* Rv: 5′-ATCTGCAGAGATGCTCCACTC-3′, *Fcgr1* Fw: 5′-GACAGTGGCGAATACAGGTGT-3′, *Fcgr1* Rv: 5′-ATGGCGACCTCCGAATCTGA-3′, *Itgam* Fw: 5′-ATGGACGCTGATGGCAATACC-3′, *Itgam* Rv: 5′-TCCCCATTCACGTCTCCCA-3′, *Ccnb1* Fw: 5′-AAGGTGCCTGTGTGTGAACC-3′, *Ccnb1* Rv: 5′-GTCAGCCCCATCATCTGCG-3′, *Ccnb2* Fw: 5′-GCCAAGAGCCATGTGACTATC-3′, *Ccnb2* Rv: 5′-CAGAGCTGGTACTTTGGTGTTC-3′, *Cdk1* Fw: 5′-AGAAGGTACTTACGGTGTGGT-3′, *Cdk1* Rv: 5′-GAGAGATTTCCCGAATTGCAGT-3′, *Cd25c* Fw: 5′-AGCGTAGCACATCTGCACATA-3′, *Cd25c* Rv: 5′-AGGAACCGTAGTAATGGGACTG-3′, *Plk3* Fw: 5′-GCACATCCATCGGTCATCCAG-3′, *Plk3* Rv: 5′-GCCACAGTCAAACCTTCTTCAA-3′,

Brca1 Fw: 5′-AGGAGGCGTCGATCATCCA-3′, *Brca1* Rv: 5′-ACAGATTTCTTTCGAGGTTGGG-3′, *Chek1* Fw: 5′-TTCCACCAACTCATGGCAGG-3′, *Chek1* Rv: 5′-GCGTTCACGATTATTATGCCGAA-3′, *Chek2* Fw: 5′-GATCATTAGCAAGCGGAGGTT-3′, *Chek2* Rv: 5′-CACCACCCGGTCAAATAGTTC-3′, *Tp53* Fw: 5′-CTCTCCCCCGCAAAAGAAAAA-3′, *Tp53* Rv: 5′-CGGAACATCTCGAAGCGTTTA-3′, *Cdkn1a* Fw: 5′-CCTGGTGATGTCCGACCTG-3′, *Cdkn1a* Rv: 5′-CCATGAGCGCATCGCAATC-3′, *Nr1h3* Fw: 5′-CTCAATGCCTGATGTTTCTCCT-3′, *Nr1h3* Rv: 5′-TCCAACCCTATCCCTAAAGCAA-3′, *Nr1h2* Fw: 5′-CGTGGTCATCTTAGAGCCAGA-3′, *Nr1h2* Rv: 5′-GCTGAGCACGTTGTAGTGGAA-3′, *Abcg1* Fw: 5′-CTTTCCTACTCTGTACCCGAGG-3′, *Abcg1* Rv: 5′-CGGGGCATTCCATTGATAAGG-3′, *Apoe* Fw: 5′-CTGACAGGATGCCTAGCCG-3′, *Apoe* Rv: 5′-CGCAGGTAATCCCAGAAGC-3′, *Pltp* Fw: 5′-CGCAAAGGGCCACTTTTACTA-3′, *Pltp* Rv: 5′-GCCCCCATCATATAAGAACCAG-3′. mRNA levels are shown as relative expression to β-actin (ΔΔCt) as indicated in figure legends.

Metabolic measurements

Seahorse assays were performed in DMEM supplemented with 2mM L-glutamine, 100 µg/ml streptomycin, phenol red and 25mM glucose + 1mM pyruvate or 5mM L-carnitine + 50 µM palmitoyl-CoA. The pH was adjusted to 7.4 with KOH. $2.5x10^5$ AMs were plated in 180µl of seahorse media per well in 3-10 replicates. Three consecutive measurements were performed under basal conditions and after the sequential addition of the following mitochondrial electron transport chain (mETC) inhibitors: 1µM oligomycin. 1µM carbonyl cyanide m-chlorophenyl (CCCP), 1µM rotenone and 1µM antimycin A (Sigma-Aldrich). Basal respiration rate (BRR)

was defined as OCR in the absence of any inhibitor. Basal ECAR (ECAR) was measured in the absence of drugs.

Lung cell suspension preparation

Adult lungs were collected in RPMI, cut into small pieces, and enzyme digested at 37ºC with Liberase TM (Sigma-Aldrich) for 30 min. Cells were passed through a 70µm cell strainer (Falcon) and washed with flow cytometry buffer. After red blood cell lysis, cells were centrifuged and resuspended in 1ml of cold flow cytometry buffer. Cells were counted with CASYton cell counter (Roche Innovatis) and stained for flow cytometry analysis.

Flow cytometry stainings

CD16/CD32 (TONBO bioscience, San Diego, CA) was used to reduce non-specific binding. The following Abs were used for the analysis of *AM surface expression profile*: anti-CD11c-Brilliant Violet 510 (HL3, BD Biosciences), anti-Siglec-F-PE, anti-Siglec-F-PerCP-Cy5.5, anti-Siglec-F-BV421 or anti-Siglec-F-Alexa Fluor 647 (All of them: clone E50-2440, BD Biosciences), anti-CD64-APC (X54-5/7.1, BD Biosciences), anti-CD11b-PE-Cy7 (M1/70, BD Biosciences), anti-CD115-biotin (AFS98, eBiosciences), Streptavidin-APC (eBiosciences). During the analysis, we realized that control $Vhl^{fl/fl}$ and CD11cΔ*Vhl* AMs had a distinct intrinsic autofluorescence (AUF), thus, we used Spectral analyzer software to normalize GMOF for each fluorochrome based on genotype-specific AUF. The following Abs were used for *lung staining*: anti-CD45-PerCP-Cy5.5 (30-F11, eBiosciences) or anti-CD45-BV570 (30-F11, Biolegend), anti-CD45.1-APC (A20, eBiosciences), anti-F4/80 biotin (BM8, Life Technologies), anti-CD11c, anti-Siglec-F, anti-CD11b, anti-I-A/I-E-FITC (2G9, BD Biosciences) or anti-I-A/I-E-APC (M5/114.15.2, BD Biosciences), anti-Ly6G-APC or anti-Ly6G-PE (1A8, BD Pharmingen), and anti-Ly6C-FITC (AL-21, BD Biosciences). The following Abs were used for *blood staining*: anti-CD45.1-APC,

anti-Ly6G-PE, anti-Ly6C-FITC and anti-CD11b-PerCP-Cy5.5 (M1/70, eBiosciences). Hoechst 33258 (Invitrogen) was used at 0.1μM as a counterstain to exclude dead cells. Lung AM population was defined as: $CD45^{+}$, $F4/80^{+}$, $CD11c^{+}$, Siglec-F^{+}, $CD11b^{-/mid}$, I-A/I-E^{lo}. Blood and lung monocytes were defined as: $CD45^{+}$, $CD11b^{hi}$, $Ly6G^{-}$, $Ly6C^{hi}$. For *intracellular Ki67 staining*, same AM number were stained for surface markers, washed twice and mixed with unstained thymocytes, used as a cell carrier. Just after, cells were fixed and permeabilized using the FoxP3 staining buffer set (eBiosciences), and then stained with anti-Ki67-eFluor 660 (SolA15, eBiosciences) or isotype control Rat IgG2aκ (eBR2a, eBiosciences). For intracellular BrdU staining, AMs were stained and mixed with carrier cells as explained above, and then fixed and permeabilized using the BrdU staining set (BD Pharmingen). Then, cells were treated with DNAse and stained with anti-BrdU Ab (BD Pharmingen).

Bioinformatics Analysis

GSE60249 array data

Gene Set Enrichment Analysis (GSEA; http://software.broadinstitute.org/gsea) was used to identify enriched gene sets from the hallmark collection of the Molecular Signature Database (MsigDB; http://software.broadinstitute.org/gsea/msigdb). Enriched gene sets were identified using a weighted enrichment statistic and a log2 ratio metric for ranking genes. Significance was defined by FDR q value < 0.25, obtained after one thousand phenotype permutations.

Heatmaps were generated with Heatmapper (Babicki et al., 2016), using no clustering method and Euclidean as distance measurement method.

RNASeq

Differential expression analysis.

Sequencing reads were pre-processed by means of a pipeline that used FastQC (www.bioinformatics.babraham.ac.uk/projects/fastqc) to assess read quality, and Cutadapt v1.6 (http://journal.embnet.org/index.php/embnetjournal/article/view/200) to trim sequencing reads, eliminate Illumina adaptor remains, and to discard reads that were shorter than 30 base pairs. The resulting reads were mapped against the mouse transcriptome (GRCm38 assembly, Ensembl release 76) and quantified using RSEM v1.2.3 (Li and Dewey, 2011). Raw expression counts were then processed with an analysis pipeline that used the Bioconductor package EdgeR (Robinson et al., 2010) for normalization (using TMM method) and differential expression testing. Only genes expressed at a minimal level of 1 count per million, in at least 3 samples, were considered for differential expression analysis. Changes in gene expression were considered significant if associated to a Benjamini and Hochberg adjusted p-value < 0.05.

Functional analysis. Collections of differentially expressed genes were analyzed with Ingenuity Pathway Analysis (https://www.qiagenbioinformatics.com/products/ingenuity-pathway-analysis) to determine significant associations to canonical pathways, biological functions and upstream transcriptional regulators; significance was defined by a Benjamini and Hochberg adjusted p-value < 0.05. GOrilla and ReViGO were used to identify and summarize Gene Ontology terms enriched in the collections of differentially expressed genes; significance was defined by FDR q value < 0.05. Venn diagram was generated by term lists comparison with Venny (http://bioinfogp.cnb.csic.es/tools/venny/index.html) to identify and visualize specific and shared elements. Circular plots representing the association between genes and enriched functional categories were generated with GOplot. GSEA was used to identify enriched gene sets, from the hallmark collection of MSigDB, having up-regulated and down-regulated genes, using a

weighted enrichment statistic and a log2 ratio metric for ranking genes. Significance was defined by FDR q value < 0.25, obtained after one thousand phenotype permutations.

BCA protein measurement

Total protein concentration was determined using Pierce BCA Protein Assay Kit (Thermo Scientific) according to the manufacturer's instruction. Albumin (Thermo scientific) was used as standard.

ELISA surfactant protein D

SP-D DUO ELISA kit and capture/detection antibodies were from R&D Systems. It was used according to manufacturer's instructions. Detection antibody was biotinylated and labeled with streptavidin-conjugated horseradish peroxidase (HRP) and visualized by incubation with 5,5′-tetramethylbenzidine solution (TMB, KPL). Reaction was stopped with TMB-stop solution (KPL). Recombinant SP-D served as standard and was included in the kit. Optical density was determined using a microplate reader (Benchmark Plus, Bio-Rad) set to 450 nm subtracting absorbance at 570 nm (wavelength correction).

Alveolar macrophage (AM) culture

- *BrdU in vitro Assay,* $2x10^5$ BAL AMs from pools of mice (n=5-6 mice per pool and genotype) were plated in triplicates (one replicate per condition: RPMI, M-CSF and rGM-CSF) in non-tissue cultured treated 24well-plates (Falcon) in 1.5 ml per well of complete RPMI and stimulated with rM-CSF and rGM-CSF (both from Peprotech) at a final concentration of 1 ng/ml and 10 pg/ml, respectively. After 12h and 36h, AMs were pulsed with BrdU at 10µM (BD Pharmingen). 24h after last pulse, cells were washed with PBS and incubated with accutase (StemCell Technologies) at 37ºC. After 20 min, cells were detached, counted and stained for surface markers and BrdU.

- *Cell morphology analysis*, $2x10^5$ AMs from individual mice (n=4-5) were cultured on crystals previously sterilized with UV radiation and placed in 24well-plates in complete RPMI at 37ºC and 5% CO_2. After 5 days, cells were fixed for 10 min with paraformaldehyde (PFA) 4% (Thermo Fisher) at RT. Crystals were stained with Hematoxylin and Eosin.

Cell image acquisition & analysis

Cells were examined with a Leica DM 2500 light microscope and images captured with a Leica DFC 420 digital camera. At least 3 images of different fields of a single mouse sample were acquired and further analyzed. Image processing and quantification of AM size and circularity were developed as a macro in Fiji (ImageJ 1.50e x64). A first preprocessing step converts the 10X color image into grayscale, applies a gaussian blurring (sigma=3), and normalizes it in order to reduce noise and standardize the intensity values. An initial segmentation of objects is done using a marker-controlled watershed algorithm (Legland et al., 2016) trying to maximize the differential detection of cells closely situated or clustered, without over-segmenting elongated cells as multiple objects. “Marker” and “mask” images used to that end were created by automatic thresholding using Minimum and Otsu implementations respectively, followed by morphological operations in order to condense the segmented objects and discard noisy elements (hole filling, closing, area opening, and removal of objects partially detected in the boundaries). The stricter first threshold allows a proper definition of seed locations (“marker”) and the more permissive Otsu method achieves robust and accurate segmentation of complete macrophages (“mask”). Objects segmented in “mask” image and split by the explained watershed strategy are later filtered to discard mistakes (dirtiness and shadows typical of the image modality), by removing those ones where the ratio between mean intensity inside the object and its 10-pixel outer-ring is lower than 120% and with dimensions very far from the typical values. Circularity

(4π*area/perimeter^2) and size are measured for each final detected cell and mean values are reported for each individual image. Statistical analysis was performed comparing average of the mean values obtained from groups of at least 5 mice per genotype and/or condition.

Supplemental References

Babicki, S., Arndt, D., Marcu, A., Liang, Y., Grant, J.R., Maciejewski, A., and Wishart, D.S. (2016). Heatmapper: web-enabled heat mapping for all. Nucleic Acids Res *44*, W147-153.

Legland, D., Arganda-Carreras, I., and Andrey, P. (2016). MorphoLibJ: integrated library and plugins for mathematical morphology with ImageJ. Bioinformatics *32*, 3532-3534.

Li, B., and Dewey, C.N. (2011). RSEM: accurate transcript quantification from RNA-Seq data with or without a reference genome. BMC Bioinformatics *12*, 323.

Robinson, M.D., McCarthy, D.J., and Smyth, G.K. (2010). edgeR: a Bioconductor package for differential expression analysis of digital gene expression data. Bioinformatics *26*, 139-140.